

# Supramolecular self-assembly of $\beta$ -cyclodextrin: an effective carrier of the antimicrobial agent chlorhexidine

Ângelo M. L. Denadai,<sup>a,b</sup> Karina I. Teixeira,<sup>c</sup> Marcelo M. Santoro,<sup>d</sup>  
Adriano M. C. Pimenta,<sup>d</sup> Maria E. Cortés<sup>b</sup> and Rubén D. Sinisterra<sup>a,\*</sup>

<sup>a</sup>Departamento de Química, Instituto de Ciências Exatas, Universidade Federal de Minas Gerais, UFMG, Avenida Antônio Carlos 6627, 31270-901, Belo Horizonte, MG, Brazil

<sup>b</sup>Centro Federal de Educação Tecnológica de Minas Gerais, CEFET-MG Uned Timóteo, MG, Brazil

<sup>c</sup>Departamento de Odontologia Restauradora, Faculdade de Odontologia, Universidade Federal de Minas Gerais, UFMG, Brazil

<sup>d</sup>Departamento de Bioquímica e Imunologia, Instituto de Ciências Biológicas, Universidade Federal de Minas Gerais, UFMG, Brazil

Received 8 September 2006; received in revised form 1 May 2007; accepted 3 May 2007

Available online 16 May 2007

**Abstract**—The supramolecular assembly between chlorhexidine and cyclomaltoheptaose ( $\beta$ -cyclodextrin,  $\beta$ CD) was characterized using NMR spectroscopy ( $^1\text{H}$ ,  $T_1$ , and ROESY), ESIMS and ITC. NMR data suggest the formation of high ordered complexes. ESIMS and ITC allowed the confirmation of the average stoichiometry as 1:4 and the thermodynamic data, also obtained by ITC, showed that the assembly is strongly stabilized by short distance interactions, but suffers a strong, opposite effect of entropy reduction. The antimicrobial activity of 1:1, 1:2, 1:3, and 1:4 Clx/ $\beta$ CD molar ratio mixtures was investigated in aqueous solution and after incorporation into mucoadhesive gels. These were used to determine the initial and the long-term antimicrobial activity, respectively, toward *Actinobacillus actinomycetemcomitans* (*A.a.*) (Y4-FDC) and *Enterococcus faecalis* (*E.f.*) (ATCC 14508) strains. The results showed that *A.a.* and *E.f.* were more susceptible to the 1:4 molar ratio mixture in either solution or gel ( $p < 0.05$ ).

© 2007 Elsevier Ltd. All rights reserved.

**Keywords:** Cyclomaltoheptaose;  $\beta$ -Cyclodextrin; Chlorhexidine; Supramolecular interactions; Antimicrobial activity

## 1. Introduction

Self-assembled<sup>1</sup> natural and synthetic systems, such as micelles, vesicles, bilayers, globular proteins, DNA, host–guest complexes, and other supramolecules, are all stabilized by non-covalent and weak interactions,<sup>2–4</sup> such as van der Waals, hydrogen bonding, ion–ion, ion–dipole, and hydrophobic effects. Controlling the assemblies is essential for constructing new materials which are more functional and have higher-ordered structures than single molecules.

Among the artificial methods for obtaining supramolecular self-assemblies, cyclomaltooligosaccharides

(cyclodextrins, CDs) are potential candidates due to their ability to form complexes with a great variety of substances, through supramolecular interactions.<sup>5–9</sup> Owing to their hydrophobic cavity, cyclodextrins as host molecules offer the guest a suitable environment for interaction. Furthermore, the outer sphere of cyclodextrins is compatible with water as a solvent, which allows hydrogen bonding cohesive interactions.<sup>5–11</sup>

Recently, we proposed that, by using seeding hydrogen bonding guest molecules, such as hydrochlorothiazide (6-chloro-3,4-dihydro-2H-1,2,4-benzothiazidine-7-sulfonamide 1,1-dioxide), at a high molar ratio of cyclomaltoheptaose ( $\beta$ CD), one could induce the self-assembly process, resulting in a high ordered complex.<sup>5</sup> Based on that we hypothesized that (i) when using guest molecules, such as the dicationic surfactant chlorhexidine (Clx, Chart 1), one could induce

\* Corresponding author. Tel.: +55 31 34995778; fax: +55 31 3499 5700; e-mail: [sinisterra@ufmg.br](mailto:sinisterra@ufmg.br)

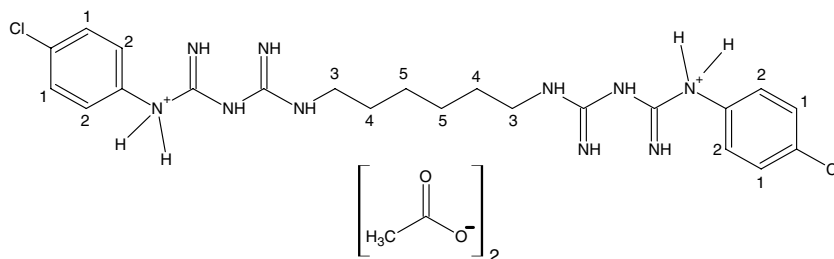


**Chart 1.** Structure of the chlorhexidine diacetate.

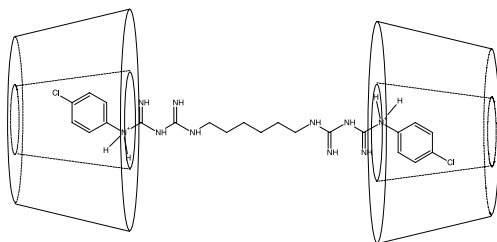


**Chart 2.** First model proposed for the chlorhexidine/βCD complex.

supramolecular self-assemblies or higher order complex formation; and (ii) if such complex is formed, one could observe higher bioavailability of the guest molecule.

Chlorhexidine [1,1'-hexamethylenebis[5-(4-chlorophenyl)-biguanide] and its salts are well known for their antibacterial activity and have been used in aqueous-based oral compositions to counter dental plaque formation and caries caused by bacteria in the oral cavity. Chlorhexidine is active against a wide range of Gram-positive and Gram-negative organisms: yeast, fungi, facultative anaerobes, and aerobes.<sup>12–14</sup>

Chlorhexidine is a strong base and is most stable in the form of salts, such as the digluconate, acetate, and dihydrochloride.<sup>12</sup> Chlorhexidine and its derivatives have the disadvantage of staining the teeth following repeated use and have furthermore a bitter taste.<sup>14–16</sup>

In a previous paper, our group described a strategy to circumvent these problems using a composition involving a 1:2 Clx/βCD molar ratio mixture,<sup>11</sup> where it was supposed that the formed complex had a 1:2 stoichiometry, based on the linear structure of Clx (Chart 2) and other results from the literature.<sup>15</sup> However, no attention was given to the possibility of self-assembly in high ordered complexes as proposed in the present work.

Thus, in order to check the above hypothesis, the supramolecular self-assembly of Clx/βCD was characterized using <sup>1</sup>H NMR, *T*<sub>1</sub>, and <sup>1</sup>H–<sup>1</sup>H 2D-ROESY, ESIMS and ITC techniques. The antimicrobial activity of the highly ordered supramolecular complex, obtained at high molar ratios of the βCD, was also considered toward *Enterococcus faecalis* ATCC 14508 and *Actinobacillus actinomycetemcomitans* Y4 FDC.

## 2. Results and discussion

### 2.1. NMR studies

NMR spectroscopy allowed the observation of the short distance interaction between Clx and βCD and the determination of the complex stoichiometry through the Job plot.

Figure 1 illustrates a comparison between the <sup>1</sup>H NMR spectra of Clx/D<sub>2</sub>O and 1:1 Clx/βCD/D<sub>2</sub>O, while Table 1 lists the chemical shift values for Clx hydrogens in the Clx/D<sub>2</sub>O and 1:1 Clx/βCD/D<sub>2</sub>O systems. The inset in Figure 1 clearly shows a sharp coalescence of the aromatic <sup>1</sup>H NMR signals of Clx in the presence of βCD and Table 1 shows changes in chemical shifts for other hydrogen atoms.

These results could be ascribed to disturbances in the electronic density of the Clx aromatic ring caused by unbounded electrons of the C-1–O-5–C-4 oxygen atoms from the glycosidic linkages of the cyclodextrin molecule, due to the formation of dipolar interactions.<sup>17,18</sup>

Chemical shift changes of the aromatic hydrogens named H-1' were used for check the stoichiometry of Clx:βCD complex by the 'Continuous Variation Method' known as Job plot.<sup>3,19</sup> The Job's plot presented in Figure 2 shows a maximal at *R* = [Clx]/([Clx] + [βCD]) = 0.4, corresponding to the 1:2 stoichiometry, showing that this is the most stable species in solution in accordance to the observations reported previously.<sup>11,15</sup>

Relaxation time measurements were carried out with the aim of monitoring the molecular mobility of Clx in the absence as well as in the presence of βCD. For organic molecules where the relaxation process occurs mainly due to the dipolar relaxation mechanism, the longitudinal relaxation time constants are inversely proportional to the molecular correlation time, *τ*<sub>c</sub>, or directly proportional to the rotational diffusion coefficient—*D*<sub>rot</sub><sup>5,6,20–22</sup>

$$T_1(\text{DD}) \propto \frac{1}{\tau_c} \propto D_{\text{rot}} \quad (1)$$

By *T*<sub>1</sub> data analysis (Table 2), it can be observed that in the presence of cyclodextrin, the *T*<sub>1</sub> values are diminished, indicating that, in this case, the molecular

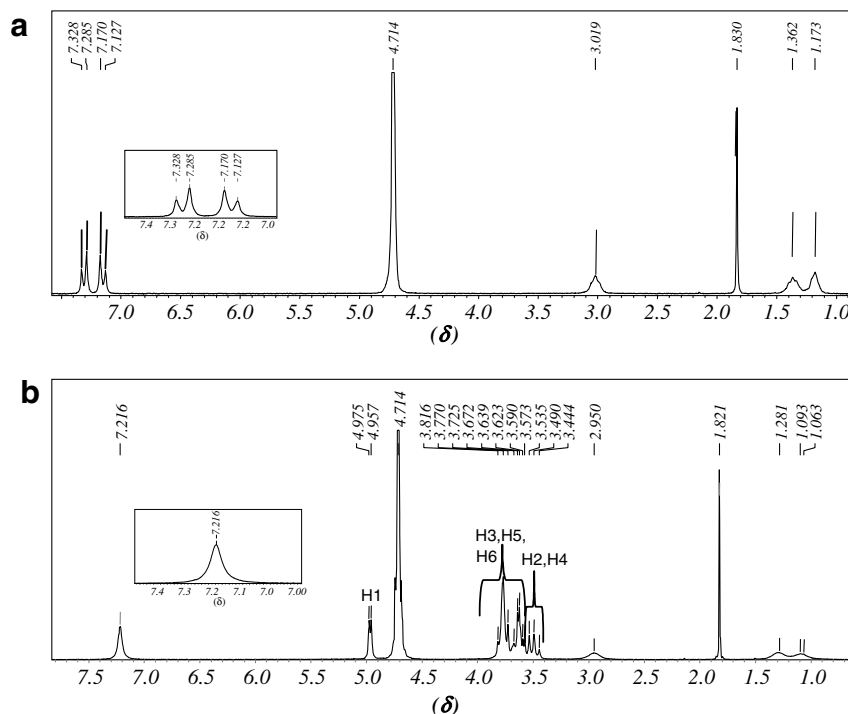


**Figure 1.**  $^1\text{H}$  NMR 200 MHz of (a) Clx/ $\text{D}_2\text{O}$ ; (b) Clx/ $\beta\text{CD}/\text{D}_2\text{O}$  (molar ratio 1:1).

**Table 1.**  $^1\text{H}$  NMR Chemical shifts<sup>a</sup> for Clx/ $\text{D}_2\text{O}$  and Clx/ $\beta\text{CD}/\text{D}_2\text{O}$  systems

H	$\delta$ Clx	$\delta$ Clx/ $\beta\text{CD}$	$\Delta\delta$	Maximal standard shift <sup>b</sup>
1'	$7.388 \pm 0.003$	$7.307 \pm 0.004$	$-0.081$	0.004
2'	$7.231 \pm 0.003$	$7.307 \pm 0.004$	$0.076$	0.004
3'	$3.099 \pm 0.006$	$3.03 \pm 0.01$	$-0.069$	0.01
4'	$1.445 \pm 0.003$	$1.367 \pm 0.003$	$-0.003$	0.003
5'	$1.255 \pm 0.004$	$1.16 \pm 0.1$	$-0.078$	0.1
a	$1.913 \pm 0.003$	$1.910 \pm 0.002$	$-0.085$	0.003

<sup>a</sup> Measured at 200 MHz for solutions of pure Clx (5.3 mM) and Clx/ $\beta\text{CD}$  (5.3 mM, 1:1 molar ratio) in  $\text{D}_2\text{O}$ .

<sup>b</sup> 'Maximal standard shift' is the sum of standard shifts of the  $^1\text{H}$  NMR experiments of pure Clx and Clx/ $\beta\text{CD}$ .

mobility is reduced. These variations in  $T_1$  can be ascribed to the complexation phenomena between Clx and  $\beta\text{CD}$ , which leads to the decrease of Clx mobility due to the formation of a new species with a new size, a new symmetry, and, consequently, a new molecular dynamics.

It is interesting to note that all Clx hydrogen atoms change their  $\delta$   $^1\text{H}$  and  $T_1$  values upon complexation with  $\beta\text{CD}$ , suggesting a more complex interaction than that

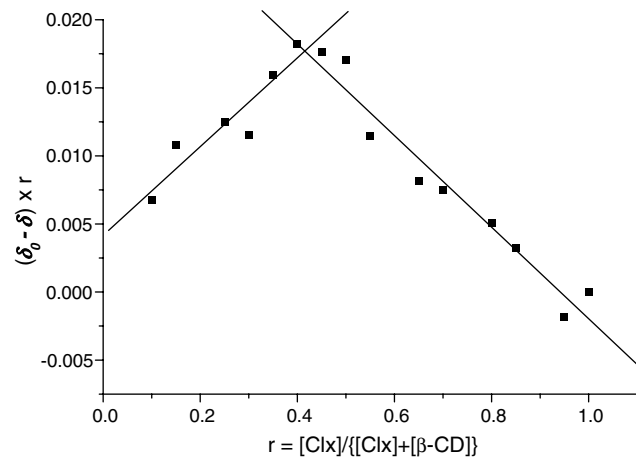


**Figure 2.** Job's plots corresponding to the chemical shift displacement of aromatic H-1'Clx hydrogen, in  $\text{D}_2\text{O}$  at 200 MHz.

resulting from the 1:2 stoichiometry, as reported in other studies.<sup>11,15</sup>

The 2D ROESY experiments allowed observation of the spatial proximity at the 5 Å maximal limit,<sup>5,6,18,23–26</sup>

**Table 2.**  $^1\text{H}$  NMR longitudinal relaxation times ( $T_1$ )<sup>a</sup> values for Clx/ $\text{D}_2\text{O}$  and Clx/ $\beta\text{CD}/\text{D}_2\text{O}$

H	1'	2'	3'	4'	5'	a
$\delta$ Clx pure	$7.388 \pm 0.003$	$7.231 \pm 0.003$	$3.099 \pm 0.006$	$1.445 \pm 0.003$	$1.255 \pm 0.004$	$1.913 \pm 0.003$
$T_1$ (s)	$1.8 \pm 0.2$	$1.8 \pm 0.2$	$0.38 \pm 0.02$	$0.35 \pm 0.01$	$0.35 \pm 0.01$	$5.0 \pm 1.0$
$\delta$ Clx/ $\beta\text{CD}$	$7.307 \pm 0.004$	$7.307 \pm 0.004$	$3.03 \pm 0.01$	$1.367 \pm 0.003$	$1.17 \pm 0.1$	$1.910 \pm 0.002$
$T_1$ (s)	$0.85 \pm 0.01$	$0.85 \pm 0.01$	$0.217 \pm 0.002$	$0.213 \pm 0.004$	$0.231 \pm 0.006$	$5.8 \pm 0.4$
$\Delta T_1$ (s)	$0.95 \pm 0.2$	$0.95 \pm 0.2$	$0.163 \pm 0.02$	$0.137 \pm 0.01$	$0.119 \pm 0.01$	$-0.8 \pm 1.0$

<sup>a</sup> Measured at 200 MHz for solutions of pure Clx (5.3 mM) and Clx/ $\beta\text{CD}$  (5.3 mM, 1:1 molar ratio) in  $\text{D}_2\text{O}$ .

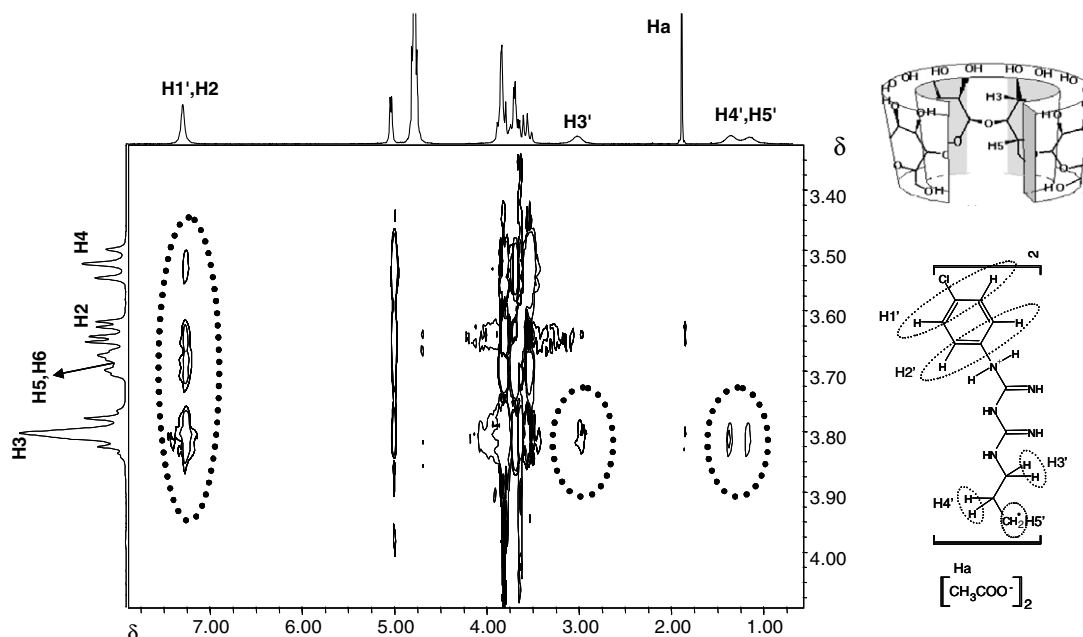


**Figure 3.** Expansion of the contour map NMR ROESY (400 MHz, D8 = 300 ms) of the Clx/βCD/D<sub>2</sub>O system.

among the functional groups of the Clx and βCD molecules. **Figure 3** shows the expansion of the contour map obtained from ROESY experiments using the Clx/βCD/D<sub>2</sub>O system at 400 MHz.

From this experiment, correlations between aliphatic and aromatic hydrogens of Clx, with H-3' and H-5' hydrogens inside the βCD cavity, could be observed. Correlations between Clx aromatic hydrogens and βCD outer hydrogens, H-4' and H-6', were also observed.

These data demonstrate the penetration of Clx into the βCD cavity as well as a simultaneous form of interaction with the outer regions of the cyclodextrin. These results corroborate the idea of the occurrence of more complicated supramolecular arrays with a stoichiometry higher than 1:2, initially reported in the literature.<sup>11,15</sup>

## 2.2. Electrospray mass spectrometry

In order to assess the species present in the Clx/βCD solution at a 1:4 molar ratio (1 mM of Clx and 4 mM of βCD), ESIMS measurements were used (**Fig. 4**). The ESI technique is not precise enough to monitor weak non-covalent interactions as this type of experiment may disturb the chemical equilibrium of the system due to the drastic conditions (high electrical field and high temperature).<sup>3,27–30</sup> For this reason, ESIMS was only used qualitatively to identify the species present in the solution.

**Figure 4** shows partner regions of the ESI experiment where *m/z* peaks corresponding to the Clx/βCD species with 1:1, 1:2, 1:3, and 1:4 stoichiometries could be observed. This is in agreement with the presence of a high ordered complex, as suggested by the NMR data. Also,

it is important to remember that solutions at low molar ratio were not detected stoichiometries greater than 1:1.

Clx is a molecule with a linear dimension of 28.55 Å, whereas the length of the βCD cavity is 7.8 Å. Thus, in terms of relative size, one can suppose that the species are present in equilibrium in solution, as illustrated in **Scheme 1**, and in this situation, an increase or decrease in the βCD concentration could be able to displace the equilibrium toward the formation of larger or smaller stoichiometries, respectively.

## 2.3. Isothermal titration calorimetry

The experiments described above suggest that in Clx/βCD systems, there are other species beyond the simple 1:2 inclusion compound. Thus, in order to assess the average stoichiometry of the complex in solution as well as its thermodynamic parameters, isothermal titration calorimetry (ITC) was performed (**Fig. 5**). Titration microcalorimetry allows for the simultaneous determination of the enthalpy, the equilibrium constant, and the stoichiometry from a single titration curve, using the least square non-linear adjustment, as put forth by the Wiseman isotherm (Eq. 2)<sup>31,32</sup>

$$\left( \frac{dQ}{d[Clx]_{tot}} \right)_P = \Delta H^0 V_0 \left[ \frac{1}{2} + \frac{1 - X_R - r}{2\sqrt{(1 + X_R - r)^2 - 4X_R}} \right] \quad (2)$$

The above equation relates the stepwise change in the heat of the system normalized with respect to Clx concentration added per injection ( $dQ/d[Clx]_P$ ), at constant pressure, to the absolute ratio of ligand to receptor

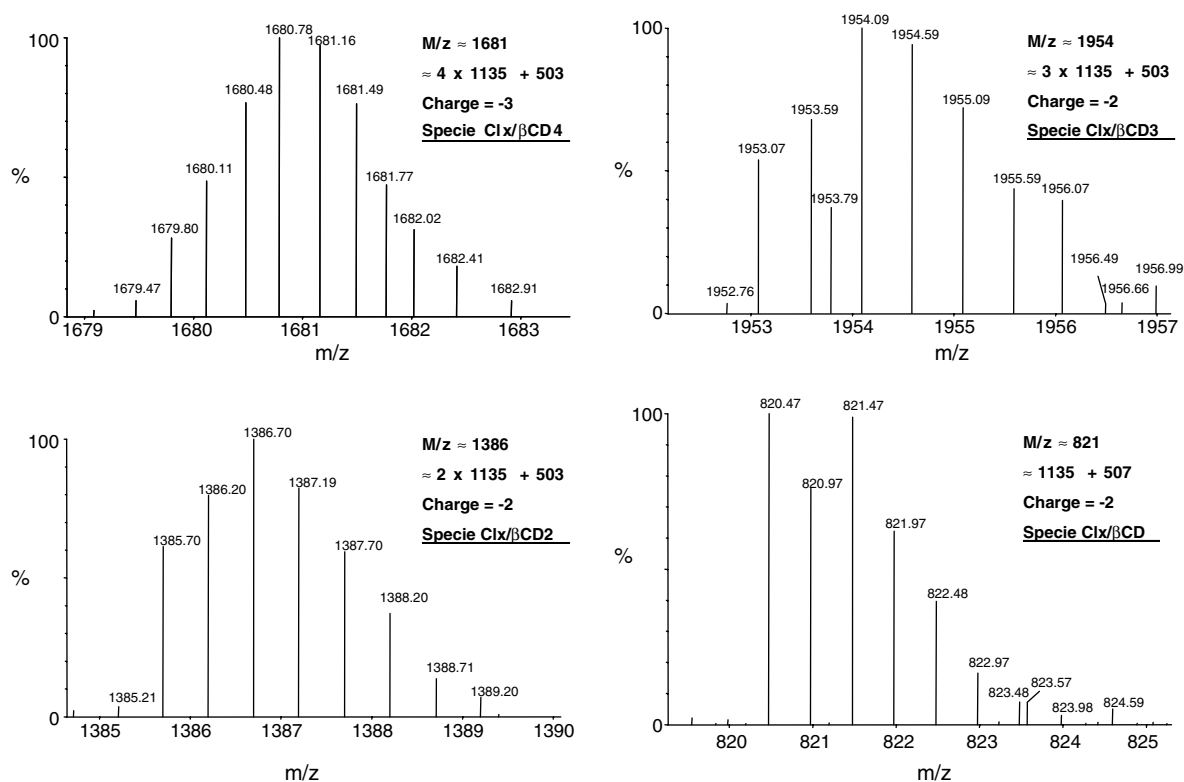
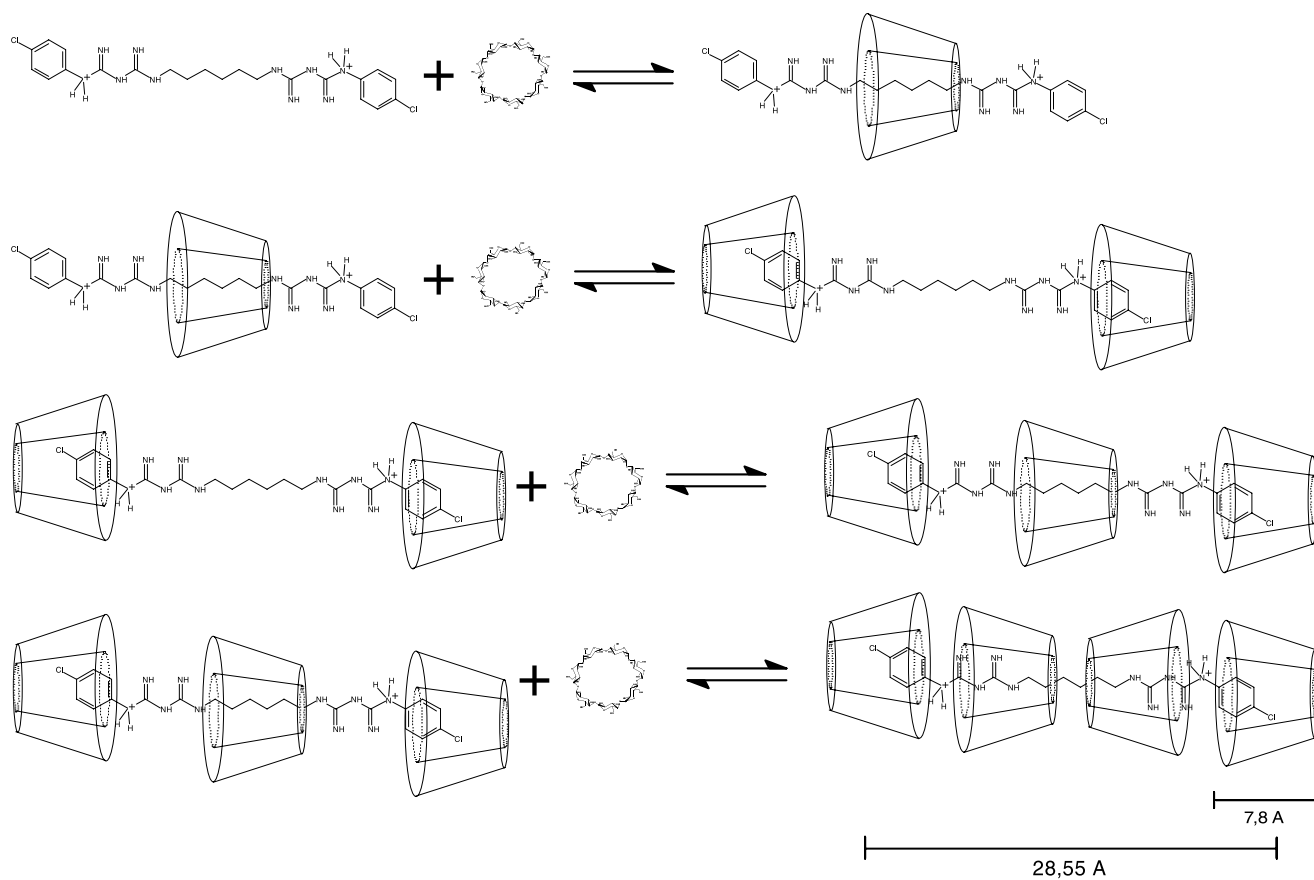
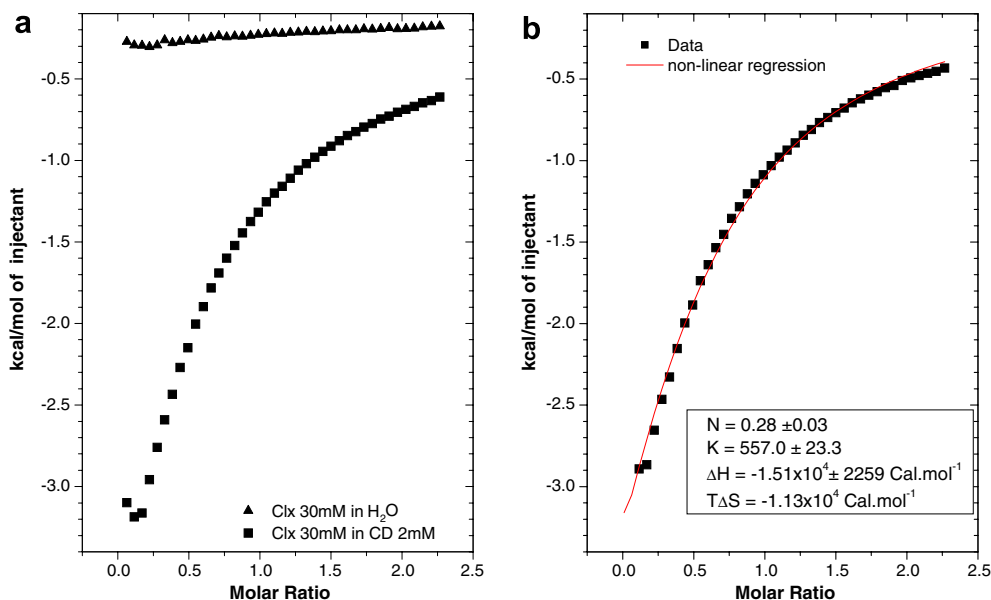


Figure 4. ESI mass spectrum of the Clx/βCD water solution.



Scheme 1. Interaction model proposed for interaction between Clx and βCD.



**Figure 5.** (a) ITC experiments for chlorhexidine (▲) in water and (■) in βCD 2 mM; (b) (■) subtracted curve of titration (—) non-linear regression of data by Eq. 2.

concentration ( $X_R = [\text{Clx}]_t / [\beta\text{CD}]_t$ ) at any point during the course of the titration. The parameters  $\Delta H^0$ ,  $V_0$ , and  $r$  are, respectively, the molar enthalpy of binding, the effective volume of the solution in the titration cell, and a composition variable  $1/[\beta\text{CD}]_t \cdot K_{\text{eq}}$ .

By using Eqs. 2 and 3, it was possible to calculate the free energy and entropy parameters:

$$\Delta G^0 = -RT \ln K \quad (3)$$

$$\Delta G^0 = \Delta H^0 - T\Delta S^0 \quad (4)$$

The experimental data for titration of Clx 30 mM in the 2 mM βCD solution, at 298.15 K, illustrated in Figure 5. The thermodynamic properties were calculated after subtracting the blank curve, as exemplified in Figure 5a and b, using the ‘one site model’ set forth by Microcal Origin 5.0 for ITC.

As depicted in Figure 5a, the Clx dilution experiment presented gradual exothermic signals in an overall range of concentrations analyzed, suggesting that this process is entropy driven due to the dilution. Titration in the βCD solution, however, presented strongly exothermic signals.

Analyzing the data from Table 3, one can check that the overall process is exothermic and compensated by

entropy decrease, which follows the same order of enthalpy variation. This demonstrates that species interact strongly by the formation of stable interactions but suffer a strong destabilization due to entropy, since the equilibrium constant is relatively low ( $K = 557$ ) when compared to other highly specific host/guest systems ( $K > 20,000$ ),<sup>31</sup> such as DNA–drug,<sup>33,34</sup> DNA–metal,<sup>35</sup> antibodies–ligand,<sup>36,37</sup> and protein–ligand.<sup>38–40</sup>

Enthalpy changes may well be due to the binding of enthalpy-rich water molecules released from the cyclodextrin cavity, together with bulk water molecules,<sup>17,41</sup> and by the formation of cooperative van der Waals, hydrogen bonding, and electrostatic interactions between positive biguanidine groups and partially negative groups at C-1–O-5–C-4.<sup>4,42,43</sup>

The reduction of entropy may be ascribed to the rigid architecture and new conformation assumed by species upon complexation, which confers greater molecular volume and smaller rotational and translational degrees of freedom when compared to pure substances. This information can be supported by the  $T_1$  NMR measurements described above. Additionally, the entropy reduction can be ascribed to the formation of a high order complex, which is compatible with the stoichiometry coefficient observed in the molar ratio of 0.27, which strongly suggests a 1:4 Clx/βCD stoichiometry.

To corroborate the average stoichiometry, the interactive ‘sequential binding site’ model, also furnished by Microcal Origin 5.0 for ITC, was applied for stoichiometry values  $N = 1, 2, 3, 4, 5$ , and 6. The optimal adjustment was considered through the analysis of the  $\chi^2$  minimization, which measures the degree of adjustment. Figure 6 shows a plot of  $\chi^2$  versus  $N$ . These data

**Table 3.** Global thermodynamic parameters<sup>a</sup> of interaction between Clx and βCD

$N$	$K_{1:1}$	$\Delta_{\text{int}}G_{1:1}$ (kJ/mol)	$\Delta_{\text{int}}H_{1:1}$ (kJ/mol)	$T\Delta_{\text{int}}S_{1:1}$ (kJ/mol)
0.28	$557 \pm 23.3$	-5.7	-63.1	-47.4

<sup>a</sup> Measured at 298.15 K.



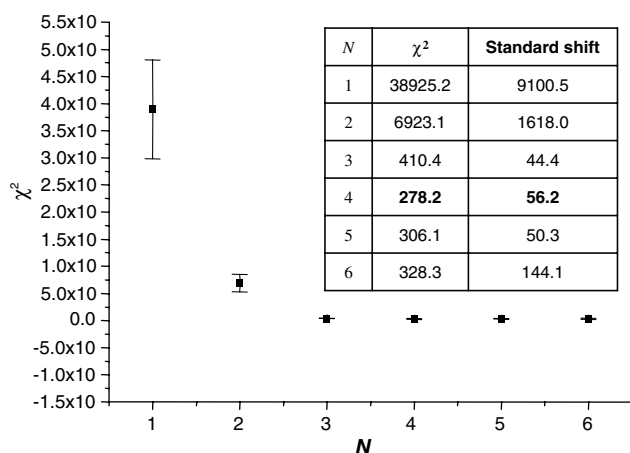


**Figure 6.** Statistical analysis of the stoichiometry coefficient using the 'sequential binding site model'.

demonstrate a better adjustment for  $N = 4$ , supporting the ITC conclusions obtained above.

Finally, to improve the inferences about the complicated process involved in the interactions, an ITC experiment was managed by injection of 12.0 mM of  $\beta$ CD into a cell charged with Clx at 0.5 mM, in order to corroborate that Clx/ $\beta$ CD relative concentrations control the structure of the complex, generating a stepwise process (Fig. 7).

As can be seen from Figure 7, the profile of the titration curve is very different from the sigmoid profile generally recorded for other ITC binding studies.<sup>31,32,36–40,44</sup> The interaction between Clx and  $\beta$ CD is initially an endothermic process, up to a molar ratio of 0.5, since the heat flow ( $dQ/d[\beta\text{CD}]$ ) is reduced

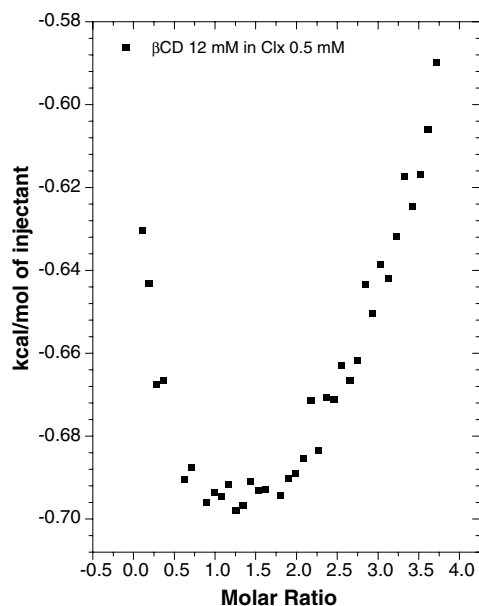


**Figure 7.** ITC experiment for titration of 12.0 mM  $\beta$ CD in 0.5 mM Clx solution.

upon injection of  $\beta$ CD. The heat flow stands approximately constant through a minimum of nearly  $-700$  kJ/mol, up to a molar ratio of 2.0. Next the heat flow increases again, due to the exothermic process. The minimal of energy up to a cyclodextrin molar ratio  $R = 2.0$  suggests more enthalpy stable species at a 1:2 Clx/ $\beta$ CD stoichiometry, corroborating the Job experiment.

These data confirm that  $\beta$ CD complexation with Clx is a stepwise process involving different species as a function of the CD concentration, resulting in the energy variations.

Analyzing the molar ratio values in Figure 7, it can be observed that the curve does not reach an asymptote and continuous injections of  $\beta$ CD are able to generate heat flow. In reality, the titration ends due to the limited solubility of  $\beta$ CD ( $\approx 15$  mM). An injectant soln of  $\beta$ CD, 12 mM, was used to make sure that no precipitation occurred during the experiments.

Thus, it is reasonable to assume that above the  $\beta$ CD/Clx (1:2) molar ratio, interaction is still verified. This result is probably due to the formation of high ordered complex or self-assembly, similar to that described elsewhere for  $\beta$ CD/guest molecules.<sup>5,8,44–46</sup> In this study stoichiometries up to 1:3 were attained, thus not excluding larger assemblies.

## 2.4. Antimicrobial evaluation

Through the physico-chemical analysis, it was possible to conclude that the structure of the Clx/ $\beta$ CD complex is molar ratio dependent. Thus, antimicrobial evaluation using different molar ratio mixtures (1:1, 1:2, 1:3, and 1:4) was tested against *E. faecalis* or *A. actinomycetemcomitans*.

The inhibition zones from bacterial inhibitions, generated by the drug for 48 h, are illustrated in Figure 8. The 1:4 Clx/ $\beta$ CD molar ratio mixture showed the highest inhibition when compared to other molar ratios and pure chlorhexidine ( $\alpha = 0.01$ ). The response for 1:3 was significantly higher when compared to free chlorhexidine. All groups, at different concentrations, showed a satisfactory antimicrobial activity. The molar ratio formulations did not decrease the initial effect of the drug.

The gels showed statistical difference among the inhibition zones of the different groups after 7 days. Higher effectiveness and long-term activity of the formulation for increased chlorhexidine and cyclodextrin concentrations were observed. *A.a.* and *E.f.* were very susceptible to the 1:4 molar ratio mixture after 7 days. In the case of free chlorhexidine, the antimicrobial activity was not different between 7 and 14 days (Figs. 9 and 10). The Clx/ $\beta$ CD gels presented better antimicrobial activity in the long-term study than did the free chlorhydrate gels for the same oral microorganism pathogens. This fact

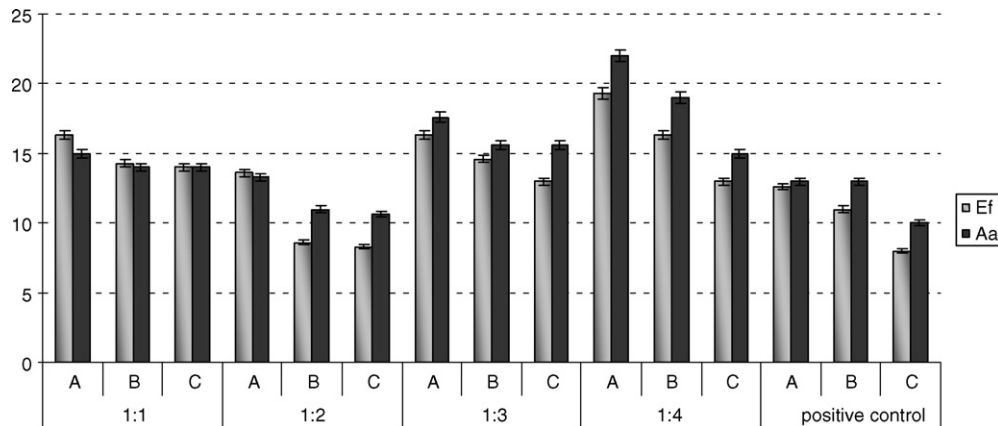


**Figure 8.** Inhibition zones (mm) of 1:1, 1:2, 1:3, and 1:4 Clx/βCD aqueous mixtures tested against *E. faecalis* and *Actinobacillus actinomycetemcomitans* after 24 h. A = 128 μg/mL, B = 64 μg/mL, and C = 32 μg/mL.

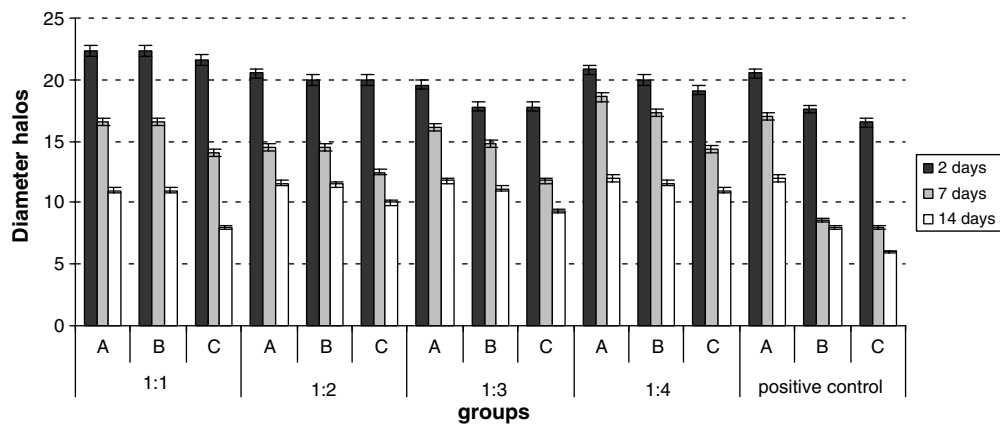


**Figure 9.** Inhibition zones (mm) of 1:1, 1:2, 1:3, and 1:4 Clx/βCD aqueous mixtures incorporated into gels tested against *Actinobacillus actinomycetemcomitans* over 14 days. A = 128 μg/mL, B = 64 μg/mL, and C = 32 μg/mL.

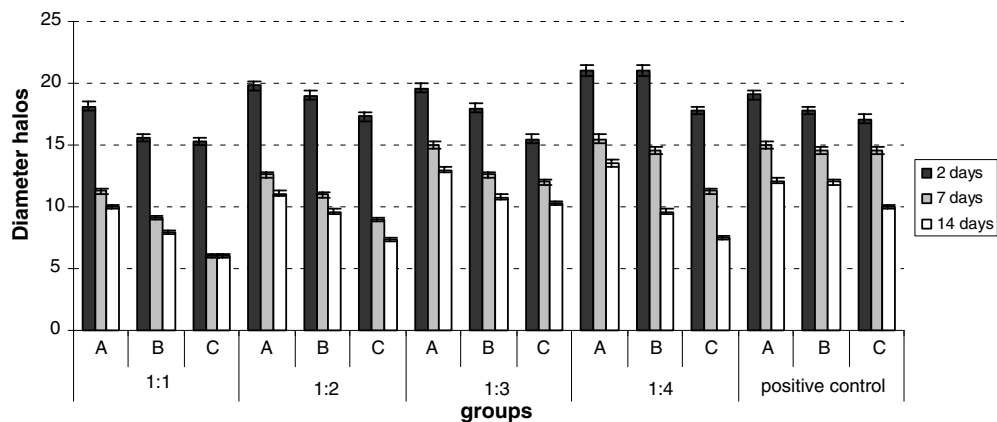


**Figure 10.** Inhibition zones (mm) of 1:1, 1:2, 1:3, and 1:4 Clx/βCD aqueous mixtures incorporated into gels tested against *Enterococcus faecalis* over 14 days. A = 128 mg/mL, B = 64 mg/mL, and C = 32 mg/mL.

was specifically noted when these formulations were tested against *A.a.*

Typically, *E.f.* is associated with recurrent infections in dentistry, showing strong resistance to antimicrobial

agents.<sup>47,48</sup> It is well known that inside dentin tubules, chemical agents in gel formulations are able to adsorb into dentin walls and increase the tissue healing capability. Similarly *A.a.* has been strongly associated with



periodontal disease and, in some cases, with destructive chronic periodontal disease.<sup>49,50</sup> The sustained release of drugs for the treatment of periodontitis disease brings a possibility for a less invasive therapy, thus allowing drug dose reduction and side effects, increasing the reinsertion of periodontal fibers, and, consequently, prolonging the longevity of the teeth.

Finally, the most appropriate concentration for solutions and gel formulations seems to be 64 µg/mL of 1:4 Clx/βCD molar ratio mixture. However, the gels presented major advantages compared to solution due to the sustained release of the active agent.

These data suggest that the 1:4 Clx/βCD molar ratio mixture can increase the concentration of the active component and that the activity of the formulation is molar ratio dependent. Thus these formulations represent an excellent option for clinical application, especially if used in endodontics or against periodontal diseases.

### 3. Experimental

#### 3.1. Materials

Chlorhexidine was obtained from E. Merck®; β-cyclodextrin from Cerestar®, Co., Milwaukee, WI, USA; hydroxymethylpropyl cellulose (HPC) from Aquapec® HV 505, Japan; Nipazol from Synth®, Brazil; Nutrient and Blood Agar from Biobrás S.A®, MG, Brazil. The microorganisms used were *E. faecalis* (*E.f*) ATCC 14508, and *A. actinomycetemcomitans* (*A.a.*) Y4 FDC, from the Federal University of Rio de Janeiro, Brazil. All other materials and solvents were of analytical grade.

#### 3.2. NMR experiments

<sup>1</sup>H NMR chemical shift ( $\delta$ ) and <sup>1</sup>H NMR longitudinal relaxation time ( $T_1$ ) experiments were obtained using a Bruker DPX-200 Avance (200 MHz) spectrometer, whereas 2D <sup>1</sup>H–<sup>1</sup>H ROESY experiments were recorded using a Bruker DRX-400 Avance (400 MHz) spectrometer, both at 300 K.

The solutions used were 5.3 mM of Clx and 5.3 mM (1:1) of Clx/βCD, both dissolved in D<sub>2</sub>O (Cambridge Isotope Laboratories, Inc—99.9% of isotopic purity). The HOD signal at  $\delta$  4.80 was used as a standard reference.

For stoichiometry complex evaluation, Job's plot was used. Briefly, solutions with different Clx/βCD molar ratios but constant total molar concentration (Clx + CD = 1 mM) were prepared.

The  $T_1$  experiments and mixing time (300 ms) for ROESY experiments were both calculated by using the inversion-recovery sequence (90– $\tau$ –180).<sup>24–26</sup> The mixing time parameter is the time interval given during each

pulse, while the evolution of dipolar coupling through space occurs among the hydrogen nuclei which remain at up to a distance of 5 Å.<sup>24–26</sup> All pulse sequences are set according to Bruker company standards.<sup>26</sup>

#### 3.3. ESIMS measurements

An ESI Micromass Q-TOF equipment was used. The data were collected from a sample of Clx/βCD at 1:4 ratio (1 mM:4 mM), using the electrospray ionization mode. The standard conditions employed included vaporization temperature 120 °C, capillary voltage 2000 V, sample cone 40 V, and extraction cone 2.0 V. The data were analyzed using the Masslynx 4.0 software from Micromass for ESI experiments.

#### 3.4. Microcalorimetric measurements

Calorimetric titrations were carried out in triplicate using a VP-ITC Microcalorimeter from Microcal at 298.15 K. The ITC instrument was previously calibrated electrically and chemically.

The studies were recorded in two ways, the first using the Clx soln as titrant and βCD in the cell, and the second, using a βCD soln as titrant and Clx in the cell.

In the first series of studies, each titration experiment consisted of 41 successive injections of the Clx aq soln (30.0 mM) into the reaction cell charged with 1.5 mL of aq βCD soln (2.0 mM), at time intervals of 540 s. The first injection of 1 µL was discarded to eliminate diffusion effects from syringe materials on the calorimetric cell. The subsequent injections were applied at a constant vol of 5 µL of Clx.

The βCD concentration in the calorimeter cell varied from 2.00 to 1.76 mM, while the concentration of the Clx varied from 0.0 to 3.5 mM. The raw data, illustrated in Figure 5, were analyzed by the software supplied together with the calorimeter (Microcal Origin 5.0 for ITC) after having subtracted the blank experiment (dilution of Clx in water). The 'one set of sites' and the 'sequential binding site' mathematic models were used to analyze the average stoichiometry.

In the second study, each titration experiment consisted of 41 successive injections of βCD aq soln (12.0 mM) into the reaction cell charged with 1.5 mL of aq Clx soln (0.5 mM). The other parameters are similar to those described above. The Clx concentration in the calorimeter cell varied from 0.5 to 0.44 mM, while the concentration of the βCD varied from 0.0 to 1.41 mM.

#### 3.5. Anti-microbial evaluation

**3.5.1. Preparation of gels.** Hydroxymethylpropyl cellulose (HPC) was dissolved in water at 3% w/v using a mechanical stirrer, at 50 °C. This gel was successfully and thoroughly mixed with the acetate of chlorhexidine

inclusion compounds (Clx/ $\beta$ CD) dissolved in propylene glycol (0.15% w/v) at 1:1, 1:2, 1:3, or 1:4 drug ratio concentration. Following complete dissolution, 0.15% (w/v) methylparaben dissolved in EtOH was added to the mixture, stirred slowly, and left for 24 h to obtain the equilibrium inside the gels. After this procedure, the air was removed by suction and the gels were stored in an amber glass flask under refrigeration (4 °C) in order to avoid drug decomposition. Positive control gels were prepared with chlorhydrate of chlorhexidine (32, 64 and 128  $\mu$ g/mL), and a plain HPC gel was used as a negative control group.

**3.5.2. Susceptibility test.** The susceptibility test of solns and gels was performed via the agar diffusion method, in accordance with the National Committee of Clinical Laboratory Standard Guidelines,<sup>51,52</sup> as regard to the drug concentration: 32  $\mu$ g/mL, 64  $\mu$ g/mL, and 128  $\mu$ g/mL (Table 1).

Strains of *E. faecalis* or *A. actinomycetemcomitans* were incubated at 37 °C in Brain Heart Infusion broth (BHI) for 24 h. A 0.1 mL aliquot of each culture of bacteria strains, prepared at a turbidity of 0.5 from the McFarland scale, was plated onto 30 mL Nutrient agar or Blood Agar, respectively. Hollows were prepared on the agar, and sterile steel cylinders were inserted and filled with 150  $\mu$ L of gel. All microorganisms were incubated at 37 °C in a reduced oxygen atmosphere. The diameters of the inhibition zones were measured and compared at intervals of 48 h over a 10 day period of incubation at 37 °C. Data obtained were analyzed by the Kruskal–Wallis non-parametric test with a significance level of  $\alpha < 0.01$ .

### Acknowledgements

The authors acknowledge financial support from the Brazilian agencies FAPEMIG, CAPES, and CNPq.

### References

- Evans, D. F.; Wennerstrom, H. *The Colloidal Domain. Where Physics, Chemistry, Biology, and Technology Meet*, 2nd ed.; WILEY-VCH: New York, 1999.
- Blokzijl, W.; Engberts, J. B. F. N. *Angew. Chem., Int. Ed. Engl.* **1993**, *32*, 1545–1579.
- Rekharsky, M.; Inoue, Y.; Tobey, S.; Metzger, A.; Anslyn, E. *J. Am. Chem. Soc.* **2002**, *124*, 14959–14967.
- Rekharsky, M. V.; Inoue, Y. *Chem. Rev.* **1998**, *98*, 1875–1917.
- Denadai, A. M. L.; Santoro, M. M.; Da Silva, L. H.; Viana, A. T.; Dos Santos, R. A. S.; Sinisterra, R. D. *J. Inclusion Phenom. Macrocycl. Chem.* **2006**, *55*, 41–49.
- Teixeira, L. R.; Sinisterra, R. D.; Vieira, R. P.; Scarlatelli-Lima, A.; Moraes, M. F. D.; Doretto, M. C.; Denadai, A. M.; Beraldo, H. *J. Inclusion Phenom. Macrocycl. Chem.* **2006**, *54*, 133–138.
- Loftsson, T.; Masson, M.; Brewster, M. E. *J. Pharm. Sci.* **2004**, *93*, 1091–1099.
- Zhang, P.; Parrotlopez, H.; Tchoreloff, P.; Baszkin, A.; Ling, C. C.; Derango, C.; Coleman, A. W. *J. Phys. Org. Chem.* **1992**, *5*, 518–528.
- Szente, L.; Szejtli, J.; Kis, G. L. *J. Pharm. Sci.* **1998**, *87*, 778–781.
- Teixeira, L. R.; Sinisterra, R. D.; Vieira, R. P.; Doretto, M. C.; Beraldo, H. *J. Inclusion Phenom. Macrocycl. Chem.* **2003**, *47*, 77–82.
- Cortes, M. E.; Sinisterra, R. D.; Avila-Campos, M. J.; Tortamano, N.; Rocha, R. G. *J. Inclusion Phenom. Macrocycl. Chem.* **2001**, *40*, 297–302.
- Basrani, B.; Lemonie, C. *Aust. Endod. J.* **2005**, *31*, 48–52.
- Zamany, A.; Safavi, K.; Spangberg, L. S. *Oral Surg. Oral Med. Oral Pathol. Oral Radiol. Endod.* **2003**, *96*, 578–581.
- Wang, L. H.; Tsai, S. J. *Anal. Chim. Acta* **2001**, *441*, 107–116.
- Qi, H.; Nishihata, T.; Rytting, J. H. *Pharm. Res.* **1994**, *11*, 1207–1210.
- Leonardo, M. R.; Tanomaru, M.; Silva, L. A. B.; Nelson, P.; Bonifacio, K. C.; Ito, I. Y. *J. Endodont.* **1999**, *25*, 167–171.
- Loftsson, T.; Brewster, M. E. *J. Pharm. Sci.* **1996**, *85*, 1017–1025.
- Schneider, H. J.; Hacket, F.; Rudiger, V.; Ikeda, H. *Chem. Rev.* **1998**, *98*, 1755–1785.
- Polyakov, N. E.; Leshina, T. V.; Hand, E. O.; Petrenko, A.; Kispert, L. D. *J. Photochem. Photobiol., A.* **2004**, *161*, 261–267.
- Levy, G. C. *Acc. Chem. Res.* **1973**, *6*, 161–169.
- Levy, G. C.; Cargioli, J. D.; Anet, F. A. L. *J. Am. Chem. Soc.* **1973**, *95*, 1527–1535.
- Breitmaier, E.; Spohn, K. H.; Berger, S. *Angew. Chem., Int. Ed. Engl.* **1975**, *14*, 144–159.
- De Alvarenga, E. S.; Lima, C. F.; Denadai, A. M. L. *Z. Naturforsch., A: Phys. Sci.* **2004**, *59*, 291–294.
- Rahman, A. *One and Two Dimensional NMR Spectroscopy*, 1st ed.; Elsevier: New York, 1989.
- Gjerde, M. I.; Nerdal, W.; Hoiland, H. *J. Colloid Interface Sci.* **1996**, *183*, 285–288.
- Werner, M. H. *Advance User's Guide, Bruker*, version 1.1 <940712>, SPECTROSPIN AG, CH-8117—Fallander: Switzerland, 1994.
- Den Brok, M. W.; van der Schoot, S. C.; Nuijen, B.; Hillebrand, M. J.; Beijnen, J. H. *Int. J. Pharm.* **2004**, *278*, 303–309.
- Zerrouk, N.; Dorado, J. M. G.; Arnaud, P.; Chemtob, C. *Int. J. Pharm.* **1998**, *171*, 19–29.
- Toma, S. H.; Uemi, M.; Nikolaou, S.; Tomazela, D. M.; Eberlin, M. N.; Toma, H. E. *Inorg. Chem.* **2004**, *43*, 3521–3527.
- Reale, S.; Teixido, E.; De Angelis, F. *Ann. Chim. (Cachan, Fr.)* **2005**, *95*, 375–381.
- Turnbull, W. B.; Daranas, A. H. *J. Am. Chem. Soc.* **2003**, *125*, 14859–14866.
- VP-ITC MicroCalorimeter, User's Manual*, 5th ed.; MicroCal® The Calorimetry Experts: Northampton, 1998.
- Barcelo, F.; Capo, D.; Portugal, J. *Nucleic Acids Res.* **2002**, *30*, 4567–4573.
- Mazur, S.; Tanious, F. A.; Ding, D.; Kumar, A.; Boykin, D. W.; Simpson, I. J.; Neidle, S.; Wilson, W. D. *J. Mol. Biol.* **2000**, *300*, 321–337.
- Xu, H.; Liang, Y.; Zhang, P.; Du, F.; Zhou, B. R.; Wu, J.; Liu, J. H.; Liu, Z. G.; Ji, L. N. *J. Biol. Inorg. Chem.* **2005**, *10*, 529–538.

36. Pancera, M.; Lebowitz, J.; Schon, A.; Zhu, P.; Freire, E.; Kwong, P. D.; Roux, K. H.; Sodroski, J.; Wyatt, R. *J. Virol.* **2005**, *79*, 9954–9969.
37. Pierce, M. M.; Raman, C. S.; Nall, B. T. *Methods* **1999**, *19*, 213–221.
38. Roberts, S. L.; Furlan, R. L.; Otto, S.; Sanders, J. K. *Org. Biomol. Chem.* **2003**, *1*, 1625–1633.
39. Lin, F. Y.; Chen, W. Y.; Sang, L. C. *J. Colloid Interface Sci.* **1999**, *214*, 373–379.
40. Perozzo, R.; Folkers, G.; Scapozza, L. *J. Recept. Signal Transduction* **2004**, *24*, 1–52.
41. Thompson, D. O. *Crit. Rev. Ther. Drug Carrier Syst.* **1997**, *14*, 1–104.
42. Rekharsky, M. V.; Yamamura, H.; Kawai, M.; Inoue, Y. *J. Org. Chem.* **2003**, *68*, 5228–5235.
43. Rekharsky, M. V.; Goldberg, R. N.; Schwarz, F. P.; Tewari, Y. B.; Ross, P. D.; Yamashoji, Y.; Inoue, Y. *J. Am. Chem. Soc.* **1995**, *117*, 8830–8840.
44. Denadai, A. M. L.; Santoro, M. M.; Lopes, M. T. P.; Chenna, A.; De Sousa, F. B.; Avelar, G. M.; Gomes, M. R. T.; Guzman, F.; Salas, C. E.; Sinisterra, R. D. *Biodrugs* **2006**, *20*, 283–291.
45. Tchoreloff, P.; Baszkin, A.; Boissonade, M. M.; Zhang, P.; Coleman, A. W. *Supramol. Chem.* **1994**, *4*, 169–171.
46. Coleman, A. W.; Nicolis, I.; Keller, N.; Dalbiez, J. P. *J. Inclusion Phenom. Mol.* **1992**, *13*, 139–143.
47. Teixeira, K. I. R.; Cortes, M. E. *Acta Odontol. Venez.* **2005**, *43*, 1–12.
48. Rams, T. E.; Listgarten, M. A.; Slots, J. *J. Periodontol. Res.* **2006**, *41*, 228–234.
49. Tavares, W. *Revis. Soc. Brasil. Med. Tropical.* **2000**, *33*, 281–301.
50. Steinberg, D.; Friedman, M.; Soskolne, A.; Sela, M. N. *J. Periodontol.* **1990**, *61*, 393–398.
51. NCCLS—National Committee for Clinical Laboratory Standards *Methods for Dilution Antimicrobial Susceptibility Tests for Bacteria that Grow Aerobically*; National Committee for Clinical Laboratory Standards: Wayne, Pennsylvania, 2000, NCCLS Document M7-A5.
52. NCCLS—National Committee for Clinical Laboratory Standards *Reference Method for Broth Dilution Antifungal Susceptibility Testing of Yeasts*; National Committee for Clinical Laboratory Standards: Wayne, Pennsylvania, 2002, NCCLS Document M27-A2.